research articles Journal of proteome research

# Proteomic Profile Regulated by the Anticancer Peptide CIGB-300 in Non-Small Cell Lung Cancer (NSCLC) Cells

**Arielis Rodríguez-Ulloa,*,† Yassel Ramos,‡ Jeovanis Gil,‡ Yasser Perera,§ Lila Castellanos-Serra,‡ Yairet García,‡ Lázaro Betancourt,‡ Vladimir Besada,‡ Luis J. González,‡ Jorge Fernández-de-Cossio,† Aniel Sanchez,‡ Joem M. Serrano,§ Hernán Farina,|| Daniel F. Alonso,|| Boris E. Acevedo,§ Gabriel Padrón,‡ Alexis Musacchio,† and Silvio E. Perea§**

*Department of Bioinformatics, Deparment of Proteomics, and Laboratory of Molecular Oncology, Center for Genetic Engineering and Biotechnology, Havana, Cuba, and Laboratory of Molecular Oncology, National University of Quilmes, Buenos Aires, Argentina*

**Received July 14, 2010**

CIGB-300 is a proapoptotic peptide-based drug that abrogates the CK2-mediated phosphorylation. This peptide has antineoplastic effect on lung cancer cells *in vitro* and *in vivo*. To understand the mechanisms involved on such anticancer activity, the NCI-H125 cell line proteomic profile after short-term incubation (45 min) with CIGB-300 was investigated. As determined by 2-DE or 2D-LC−MS/MS, 137 proteins changed their abundances more than 2-fold in response to the CIGB-300 treatment. The expression levels of proteins related to ribosome biogenesis, metastasis, cell survival and proliferation, apoptosis, and drug resistance were significantly modulated by the presence of CIGB-300. The protein translation process was the most affected (23% of the identified proteins). From the proteome analysis of the NCI-H125 cell line, novel potentialities for CIGB-300 as anticancer agent were evidenced.

**Keywords:** Comparative proteomic analysis • CIGB-300 • ribosome biogenesis • apoptosis • casein kinase 2 • nucleophosmin • lung cancer

## Introduction

Casein Kinase 2 (CK2) is a serine/threonine protein kinase overexpressed in a variety of solid and hematopoietic tumors.[1−3] In particular, lung cancer has been shown to exhibit high levels of CK2 activity and mRNA expression.[4,5] This kinase phosphorylates a wide range of substrates related to gene expression, cell survival, and apoptotic pathways; its increased expression in tumor cells promotes cellular proliferation and suppresses apoptosis.[6] Previous findings have suggested the potential of CK2 as an attractive anticancer target.[7] Therefore, to inhibit the CK2 activity, different emergent approaches have been assayed so far: (a) down-regulation of CK2 gene expression by antisense oligonucleotide,[8] (b) allosteric inhibition of the enzyme,[9] and (c) blocking of ATP binding site by small compounds.[10] CIGB-300 (formerly P15-Tat) is a novel hypothesis-driven peptide that abrogates the CK2-mediated phosphorylation by its ability to bind the substrate's phosphoaceptor domain instead of the enzyme per se.[11]

The antineoplastic effect of CIGB-300 has been well documented both *in vitro* and *in vivo* by using different cancer cell lines and mouse models.[11−13] In particular, lung cancer cells have been shown to be sensitive to CIGB-300 *in vitro* and *in vivo*. For instance, the cell viability on human non-small cell lung cancer (NSCLC) NCI-H125 and on murine lung transformed epithelial TC-1 cells were similarly reduced ($IC_{50} = 70$ $\mu$M),[11,12] and the caspase activation was detected after 30 min of CIGB-300 addition.[11] Likewise, CIGB-300 induced massive apoptosis after 10 min upon addition of 100 $\mu$M CIGB-300 to small cell lung cancer (SCLC) NCI-H82 cells.[13] *In vivo*, CIGB-300 was able to elicit significant antitumor activity both in murine TC-1 and human NCI-H125 implanted tumors.[11,13] CIGB-300 has been already studied in the clinical ground, demonstrating safety, tolerability, and efficacy signs in women with cervical malignancies.[14]

Significant advances have been made in proving the CIGB-300 mechanism of action in lung cancer cells. Recently, the nucleolar chaperone nucleophosmin (B23/NPM) has been described as the major CK2-substrate targeted by CIGB-300.[15] Such interaction inhibited the CK2-mediated phosphorylation on B23/NPM in a dose-dependent manner and led to nucleolar disassemble with subsequent apoptosis.[15] Accumulated evidence suggests that CIGB-300 could ultimately induce apoptosis by impairing the ribosome biogenesis.[15] A detailed description of differential protein expression of cells treated with CIGB-300 is needed to support the proposed mechanism of action for such peptide.

* To whom correspondence should be addressed. Department of Bioinformatics, Center for Genetic Engineering and Biotechnology, P.O. Box 6162, Havana CP10600, Cuba. Phone: 53-7271-6221. Fax: 53-7271-8070. E-mail: arielis.rodriguez@biocomp.cigb.edu.cu.

† Department of Bioinformatics, Center for Genetic Engineering and Biotechnology.

‡ Department of Proteomics, Center for Genetic Engineering and Biotechnology.

§ Laboratory of Molecular Oncology, Center for Genetic Engineering and Biotechnology.

|| National University of Quilmes.

In this work, the proteome of the nuclear fraction from NCI-H125 cells modulated by CIGB-300 was described. Two complementary proteomic techniques, two-dimensional electrophoresis (2-DE) and two-dimensional liquid chromatography coupled to tandem mass spectrometry (2D-LC−MS/MS), were used. The analysis of differentially expressed proteins suggested that CIGB-300 impair the ribosome biogenesis on these cells. Data provided here not only indicate that this peptide regulates different relevant biological processes in cancer but also set the molecular basis for a synergistic interaction with anticancer drugs.

## Materials and Methods

**Peptide.** CIGB-300 is a cyclic peptide (CWMSPRHLGTC) fused to the cell penetrating peptide Tat ($^{48}$GRKKRRQRRRPPQ$^{68}$).[11] The CIGB-300 peptide was synthesized on solid phase and purified by reverse phase high performance liquid chromatography (RP-HPLC) to >95% purity on an acetronitile/$H_2O$−trifluoroacetic acid gradient[16] and confirmed by electrospray mass spectrometry (Micromass, U.K.).

**Cell Culture and Treatments.** The non-small cell lung cancer (NSCLC) cell line NCI-H125, kindly provided by Dr. Eduardo Suarez (Center for Molecular Immunology, Havana, Cuba), was originally obtained from ATCC (Rockville, MD). The NCI-H125 cells were cultured in RPMI 1640 (Life Technologies, USA) supplemented with 10% fetal bovine serum (FBS; PAA, Canada) and 100 $\mu$g/mL gentamicin (Sigma, USA), at 37 °C in a humidified atmosphere containing 5% $CO_2$.

For proteomic analysis, $20 \times 10^6$ tumor cells were seeded in appropriate vessels and incubated for 24 h. The cells were incubated with 200 $\mu$mol/L of CIGB-300 during 45 min, taking into account that CIGB-300 induces cell death features after 60 min of incubation. For Western blot analysis, cell cultures were treated with 40, 80, or 200 $\mu$mol/L of CIGB-300 for 45 min.

**Isolation of Nuclear Proteins.** NCI-H125 cells were collected by trypsinization. After washing with phosphate buffered saline (PBS), the cells were suspended in 500 $\mu$L of the isotonic buffer containing 10 mM HEPES-NaOH adjusted to pH 7.5, 0.25 M sucrose, 1 mM EGTA, and protease inhibitors.[17] For plasma membrane solubilization Triton X-100 at final concentration of 0.25% was added. After 15 min at 4 °C, the cell lysate was centrifuged for 15 min at 12,000 × *g* and 4 °C. Nuclear pellet was washed with 500 $\mu$L of a solution containing 10 mM HEPES-NaOH, pH 7.5, 0.34 M sucrose, 0.75 mM spermidine, 0.15 mM spermine, 1 mM EDTA, 0.1% Triton X-100, and protease inhibitors, centrifuged at 1000 × *g* for 5 min at 4 °C, and decanted. Nuclear proteins were then solubilized in a lysis solution containing 7 M urea, 2 M thiourea, 2% CHAPS, 0.5% ASB-14, 15% glycerol, 2% DTT, and protease inhibitors. The suspension was sonicated (2 × 1 min) and incubated 1 h at room temperature. Free cysteines were blocked with 4% acrylamide during 1 h at room temperature. Anfolytes range 3−10 were added at 2% final concentration and DNA was removed by centrifugation at 60,000 × *g* during 3 h. The supernatant containing solubilized nuclear proteins was conserved at −70 °C for 2-DE and 2D-LC−MS/MS analysis.

**Two-Dimensional Gel Electrophoresis (2-DE).** For both nuclear fractions, treated and nontreated with CIGB-300, three replicate analytical gels and two preparative gels were run. 2-DE was performed by combining IEF in IPG for the first dimension and SDS-PAGE for the second dimension. IPG strips (p*I* range 4−7, 18 cm) (Amersham Pharmacia, Sweden) were rehydrated overnight in 350 $\mu$L of lysis solution containing 2% of anfolytes range 4−7 and approximately 400 $\mu$g of nuclear proteins for analytical gels or 700 $\mu$g for preparative gels. Electrofocusing was done at 20 °C in a Multiphor II equipment (Amersham Pharmacia, Sweden) at 50 kV-h under silicone oil. For the second dimension, IPG strips were incubated for 15 min in 3 mL of equilibration solution (6 M urea, 30% glycerol, 2% SDS, 50 mM Tris-HCl, pH 8.8). The focalized proteins were transferred to 16.8% polyacrylamide-SDS gels (prepared 24 h before use) and were run at 16 mA for 30 min and then at 30 mA for 6 h. For analytical gels, silver staining was used for detection, while preparative gels were silver stained with a MS compatible procedure.[18,19]

**2-D Image Analysis.** Images from 2-D gels were processed and analyzed using the Melanie 5 software (GeneBio, Switzerland). Spots were automatically detected without previous contrast enhancement, followed by manual editing when necessary. For each class, gel reproducibility was evaluated by using the available tools (pair reports and scatter plot analysis). Heuristic clustering was used for automatic classification of the set of gels. The detection of changes in protein maps between the two classes was first done by automatic analysis and confirmed by visual inspection of the series of gels. Histograms for groups based on percent volume of the spots were recorded, using the central tendency as the mean value and the mean square deviation as the dispersion value. The spots displaying a change in their expression between the classes greater than the 2-fold factor (determined from the mean) were considered for protein identification by MS. For molecular mass and p*I* estimation according to the protein migration in 2D gel, several intense and well-resolved spots corresponding to different gel zones were selected as landmarks. Theoretical mass and p*I* were calculated from the sequence of the identified proteins using the Compute pI/$M_w$ ExPASy tool (http://ca.expasy.org/tools/pi_tool.html).

**In-Gel Trypsin Digestion and Protein Identification. In-Gel Digestion.** Replicate spots from two preparative gels were pooled and silver staining was removed with Farmer's reagent.[20] Spots were cut in 1−3 mm$^3$ pieces, dried with acetonitrile, rehydrated in a minimum volume of ammonium bicarbonate (25 mM) containing trypsin (12.5 ng/$\mu$L, Promega, USA), and digested at 37 °C for 18 h.

**MS Analysis.** Tryptic peptides from selected spots were obtained and processed as described by González et al.[21] ESI−MS spectra were acquired using a QTof-2 hybrid type orthogonal tandem mass spectrometer (Micromass, U.K.) fitted with a Z-spray nanoflow electrospray ion source operated at 80 °C with a drying gas flow at 50 L/h. Peptides eluted with 60% ACN in 1% formic acid from ZipTips (Millipore, USA) were loaded into the borosilicate nanoflow tips. Capillary and cone voltages of 900 and 35 V were applied, respectively. To acquire the ESI−MS/MS spectra, the first quadrupole was used to select the precursor ion within a window of approximately 2 Th. Argon was used in the collision chamber at $3 \times 10^{-2}$ Pa pressure and collision energies between 25 and 50 eV were set to fragment precursor ions. Data acquisition and processing were performed using MassLynx v3.5 (Micromass, U.K.).

**Protein Identification.** Queries were done to sequence databases (Swiss-Prot and NCBI) by MASCOT search engine software.[22] Monoisotopic masses of tryptic peptides were used to identify the proteins by peptide mass fingerprinting (PMF), and additionally the most intense signals observed in every spectrum were sequenced by collision induced dissociation and ESI−MS/MS. The MS/MS ion search option of the MASCOT

program was used for protein identification; no taxonomic restrictions were made. Cysteine propionamide was considered as fixed modification. Variable modifications including deamidation of glutamine and asparagine, and methionine sulfoxide were taken into account. Other restrictions to MASCOT were precursor and fragment ions $m/z$ tolerance of 0.2 Da, enzyme digestion with trypsin, and up to one missed cleavage. Additionally, MS/MS spectra of proteins identified on the basis of sequencing of one or two peptides were manually interpreted, looking for four or more intense consecutive C-terminal $y_n''$ fragment ions and the complementary b fragment series.

**Proteomic Analysis by Two-Dimensional Liquid Chromatography Coupled to Tandem Mass Spectrometry (2D-LC−MS/MS). Trypsin Digestion.** The nuclear protein extracts, previously reduced and alkylated as described above, of control (400 $\mu$g) and CIGB-300-treated NCI-H125 cells (400 $\mu$g) were precipitated with acetone/TCA and independently dissolved in 300 $\mu$L of buffer containing 50 mM ammonium bicarbonate, 2 M urea, pH 8.0. In the case of the treated sample, the buffer was prepared in $^{18}$O-labeled water. Proteins were digested by two additions of trypsin at an enzyme-to-substrate mass ratio of 1:100, for 16 h for each one, at 37 °C. To inhibit trypsin activity and to stop the proteolytic digestion, samples were reduced and alkylated using the previously described protocol. Both digests were mixed and desalted before cation exchange chromatography.

**2D-LC−MS/MS Analysis.** A combination of strong cation exchange and reversed phase chromatography steps were used to separate the complex mixture of peptides prior to tandem mass spectrometry analysis (MS/MS). Desalted peptides were separated into 14 fractions using a 0.8 mm × 50 mm SCX II column (Agilent, USA) and NaCl gradient (from 0 to 500 mM in 100 min). Collected fractions were lyophilized and further dissolved in 130 $\mu$L of 1% formic acid. For each fraction three replicate aliquots of 40 $\mu$L were separated in independent LC−MS/MS experiments by reverse phase chromatography. Data dependent acquisition MS/MS spectra of the eluted peptides were acquired in three $m/z$ ranges (400−600, 590−900, or 890−2000). Peptides were separated and identified using an Agilent 1100 series nano LC system (Agilent, USA) coupled online to a QTof-2 hybrid mass spectrometer (Micromass, U.K.). The capillary and cone voltages of the electrospray ionization source were operated with 2.4 kV and 45 V, respectively. Samples were applied at 20 $\mu$L/min to an LC-Packings PepMap C18 Precolumn Cartridge (5 mm × 300 $\mu$m i.d.) for 10 min and then switched onto a C18 capillary column (15 cm × 75 $\mu$m i.d., packed with 5 $\mu$m, Zorbax 300 SB) using a mobile phase containing 0.1% formic acid, 5−45% acetonitrile gradient over 90 min at 300 nL/min flow rate. For protein identification, 1 s survey scans were acquired over the selected mass range and a maximum of 4 concurrent MS/MS acquisitions were triggered for 2+, 3+ charged precursors ions detected at an intensity above a 15 counts/s threshold. Each MS/MS acquisition was completed and switched back to MS mode when the total ion current fell below a 2 counts/s threshold or after a maximum of 6 s of continuous acquisition.

**Data Analysis.** Raw files were processed using MASCOT Distiller 2.3 software. Peptides were assigned to MS/MS spectra using MASCOT search engine against the IPI human database (version 3.61). The following search parameters were selected: 2 Da precursor mass tolerance, 0.8 Da MS/MS ions mass tolerance, tryptic search with up to one missed cleavage, oxidized methionine as variable modification, and cysteine propionamide as fixed modification. To accept a peptide hit as positive we considered a false discovery rate (FDR) of 3% based on the target-decoy strategy.[23]

Quantification was achieved using ISOTOPICA software.[24,25] The software enables the relative peptide quantification based on the detailed analysis of the observed isotopic ion distribution. The software calculates the best ratio of the nonlabeled ($^{16}O_2$, control condition) and labeled ($^{18}O_1 + {}^{18}O_2$, treated with CIGB-300) to obtain an *in silico* isotopic ion distribution that best match with the observed experimentally. To evaluate the quality of this adjustment, the software calculates the area difference between both isotopic ion distributions, and it is expressed as a coefficient named GOF (goodness of fitting). The relative quantifications of peptides with GOF below 0.6 were not considered for further analysis. All relative quantifications were additionally manually inspected.

**Western Blot Analysis.** Treated cells were collected by standard trypsinization and subsequently lysed using RIPA buffer (BDH, Germany) according the supplier's recommendations. Then, the cellular lysate was cleared by centrifugation at 12,000 rpm during 15 min at 4 °C and quantified by the Bradford assay (Bio-Rad, USA). Protein samples were loaded into individual SDS-PAGE wells (5 $\mu$g of total protein/well), electrophoretically resolved, and transferred to a nitrocellulose membrane. The membrane was blocked 4% skimmed milk in PBS, for 18−20 h at 4 °C. Then, 1 $\mu$g/mL of either antinucleophosmin (B23/NPM) monoclonal antibody (Zymed, USA) or antiprohibitin (PHB) rabbit polyclonal antibody (Sigma, USA) was added and incubated for 1 h at 37 °C. After washing with PBS, the membrane was incubated with antimouse IgG (1:1000) or antirabbit IgG polyclonal (1:1000) secondary antibodies conjugated to horseradish peroxidase (Sigma, USA). Finally, the antigen−antibody reaction was developed using enhanced chemiluminescence (Amersham Life Science, USA), according to the instructions of the manufacturer.

**Bioinformatics Analysis.** Functional classification of identified proteins was based on the information annotated in the Gene Ontology (GO) database (http://www.geneontology.org). The analysis was performed using the DAVID functional annotation tool (http://david.abcc.ncifcrf.gov/).[26,27] Biological pathways associated with differentially expressed proteins were identified by using the functional enrichment tool ToppFun.[28] During this analysis, ToppFun retrieves information from databases such as BioCyc (http://biocyc.org/), Panther (http://www.pantherdb.org/), Reactome (http://www.reactome.org/cgi-bin/frontpage?DB=gk_current), Kyoto Encyclopedia of Genes and Genome (KEGG, http://www.genome.jp/kegg/pathway.html) and MSigDB (http://www.broadinstitute.org/gsea/msigdb/). The software computes Bonferroni correction to identified significant enriched pathways ($p$-values lower than 0.05), as statistical analysis. Proteins associated with the enriched pathways were visualized in a network context using the Cytoscape software (version 2.6.0).[29]

## Results and Discussion

CIGB-300 is a peptide-based drug that has just started to be explored at the clinical level. The first data concerning safety and efficacy signs in women with cervical malignancies have been already reported.[14] As lung cancer cells have shown to be highly sensitive toward CIGB-300 anticancer effect either *in vitro*[11,12,15] or *in vivo*,[13] these tumors become an attractive target for clinical testing of CIGB-300. The nuclear proteome regulated in the presence of 200 $\mu$M of CIGB-300 was then

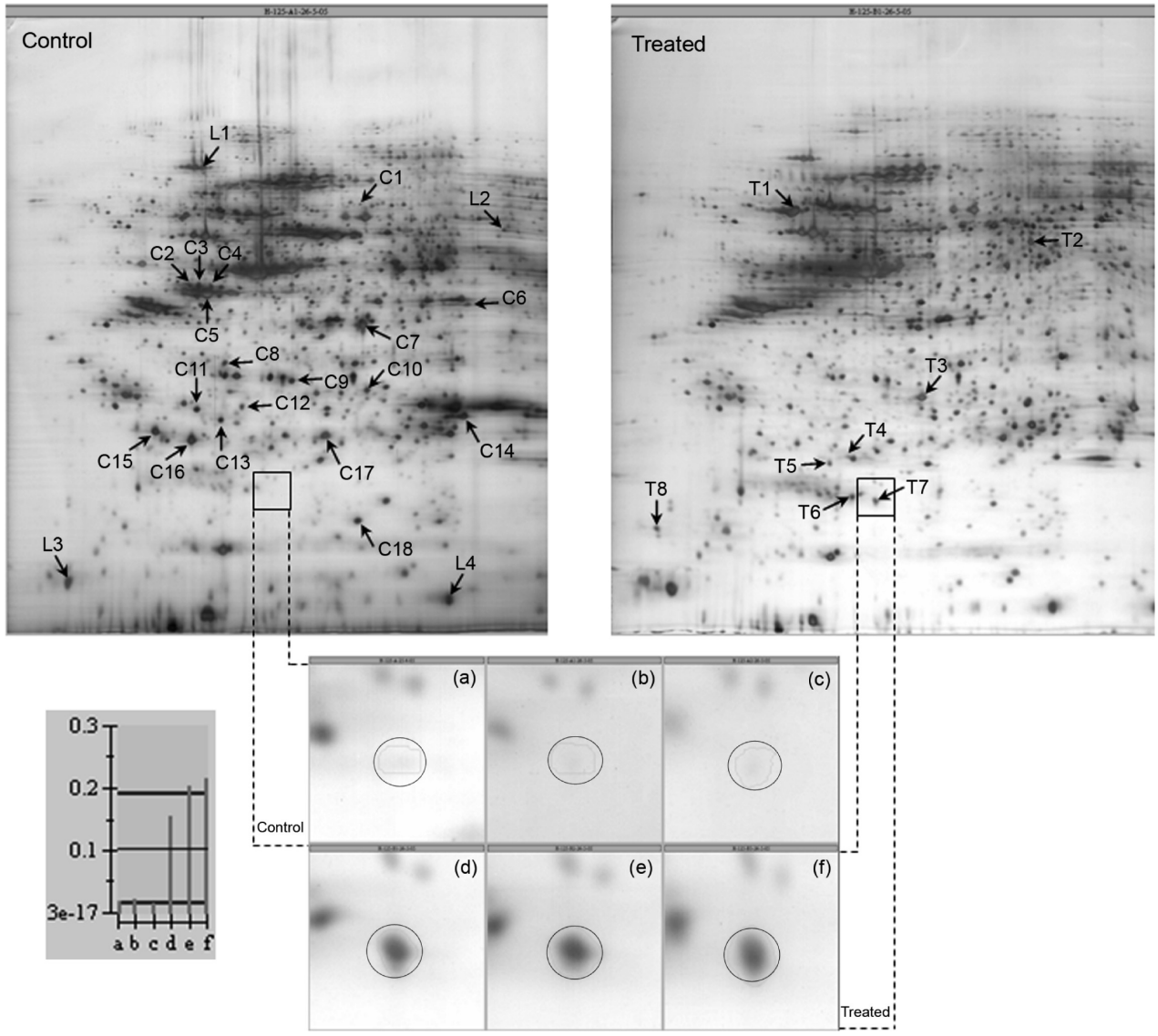


**Figure 1.** Representative bidimensional electrophoresis gels derived from control and CIGB-300 treated cells. Proteins were separated by combining IEF in IPG (p*I* range from 4 to 7) and SDS-PAGE (mass range from 12 to 120 kDa). Arrows indicate 26 spots significantly modulated (fold change >2) by CIGB-300 treatment. The magnified regions (a−c, control condition; d−f, treated cells) show the effect of CIGB-300 on the spot coded as T7 corresponding to nucleophosmin (B23/NPM) fragment. The histogram of three replicates for each conditions (a−f) is shown at the left of the magnified regions.

studied using the NCI-H125 lung cancer cell line as target cells. Studies on the permeability of CIGB-300 have indicated that such peptide dose represents the inhibitory concentration 90 ($IC_{90}$) for CIGB-300 in NCI-H125 cells, which guarantees the full biological activity and better intracellular uptake in more than 90% of the cells (unpublished observations).

In a first approach, 2-DE in conjunction with quantitative image analysis and sequencing by mass spectrometry was used to investigate the CIGB-300 modulated protein profile. The Figure 1 shows the 2-D pattern for nuclear proteins of NCI-H125 cells cultured with CIGB-300 or medium alone during 45 min. Between 1600 and 2000 spots were detected by image analysis in the three replicate analytical gels of each condition. A total of 26 differentially expressed spots were subjected to trypsin digestion and mass spectrometry analysis. The 22 identified proteins that were up- or down-regulated more than 2-fold after treatment with CIGB-300 are shown in Table 1. The apparent relative molecular weight ($M_r$) and the isoelectric point (p*I*) determined from 2-D calibrated gels for the identified proteins were compared with their corresponding theoretical values. With the exception of LIM and SH3 domain protein 1 (LASP1) and B23/NPM protein, all of the identified proteins revealed good correlation between both values (Table 1).

In the case of LASP-1 protein, the $M_r$ of 36.4 kDa and p*I* of 6.2 were detected in 2-D gels, similar to 34.5 kDa and p*I* 6.3 values, previously reported.[30] Two spots (T8 and T7), with $M_r$ of 16.0 and 17.7 kDa, corresponding to B23/NPM fragments were identified on CIGB-300-treated cells (Figure 1). This finding suggested that CIGB-300 could promote partial B23/NPM degradation in the experimental condition, a relevant observation, as such a protein was reported to be a major target for CIGB-300.[15] Given the fact that B23/NPM stability is increased by its CK2-mediated phosphorylation[31] along with the ability of CIGB-300 to abrogate such a process,[15] B23/NPM degradation is expected to occur, and it represents a subrogated marker of CIGB-300 functionality. However, a decreased ex-

**Table 1.** Differentially Expressed Proteins in NCI-H125 Cells Treated with CIGB-300, Identified Using 2-DE and Mass Spectrometry Approach

| spot no. | UniProt_ACC[a] | description | gene symbol[b] | % coverage (matching peptides)[c] | $M_r$ (kDa)[d] | p$I$[d] | FC[e] |
|---|---|---|---|---|---|---|---|
| | | Apoptosis | | | | | |
| T3 | P35232 | Prohibitin | PHB | 51 (13) | 29.8−**26.1** | 5.6−**5.5** | 2.5 |
| T7 | P06748 | Nucleophosmin (fragment) | NPM1 | 36 (6) | 32.6−**17.7** | 4.6−**5.3** | 11.0 |
| T8 | P06748 | Nucleophosmin (fragment) | NPM1 | 23 (6) | 32.6−**16.0** | 4.6−**4.2** | 8.0 |
| C11 | P52565 | Rho GDP-dissociation inhibitor 1 | ARHGDIA | 30 (3) | 23.1−**24.6** | 5.0−**4.9** | −5.3 |
| C15 | P13693 | Translationally controlled tumor protein | TCTP | 65 (6) | 19.6−**22.6** | 4.8−**4.7** | −5.2 |
| C16 | Q04760 | Lactoylglutathione lyase | GLO1 | 84 (17) | 20.6−**21.9** | 5.1−**4.9** | −4.5 |
| C17 | P09211 | Glutathione S-transferase P | GSTP1 | 66 (14) | 23.2−**22.3** | 5.4−**5.5** | −3.1 |
| C18 | P00441 | Superoxide dismutase | SOD1 | 44 (5) | 15.8−**16.2** | 5.7−**5.7** | −6.8 |
| | | Cell proliferation | | | | | |
| T2 | O60884 | DnaJ homologue subfamily A member 2 | DNAJA2 | 50 (12) | 45.7−**44.5** | 6.1−**6.0** | 3.0 |
| | | Glucose catabolic process | | | | | |
| C7 | P07195 | L-lactate dehydrogenase B chain | LDHB | 35 (10) | 36.5−**33.7** | 5.7−**5.7** | −3.8 |
| C14 | P60174 | Triosephosphate isomerase | TPI1 | 54 (11) | 26.5−**23.9** | 6.5−**6.2** | −2.9 |
| | | RNA processing | | | | | |
| C1 | P61978 | Heterogeneous nuclear ribonucleoprotein K | HNRNPK | 20 (6) | 51.0−**53.0** | 5.4−**5.7** | −3.2 |
| C2 | P07910 | Heterogeneous nuclear ribonucleoproteins C1/C2 | HNRNPC | 23 (7) | 33.5−**39.2** | 4.9−**4.8** | −16.9 |
| C3 | P07910 | Heterogeneous nuclear ribonucleoproteins C1/C2 | HNRNPC | 39 (10) | 33.5−**39.2** | 4.9−**4.9** | −13.9 |
| C4 | P07910 | Heterogeneous nuclear ribonucleoproteins C1/C2 | HNRNPC | 18 (5) | 33.5−**39.0** | 4.9−**5.0** | −11.7 |
| C5 | P07910 | Heterogeneous nuclear ribonucleoproteins C1/C2 | HNRNPC | 32 (12) | 33.5−**37.8** | 4.9−**5.0** | −3.0 |
| | | Regulation of transcription | | | | | |
| T4 | P45973 | Chromobox protein homologue 5 | CBX5 | 24 (4) | 22.2−**20.7** | 5.7−**5.1** | 5.4 |
| T6 | Q13185 | Chromobox protein homologue 3 | CBX3 | 44 (5) | 20.8−**18.2** | 5.2−**5.1** | 3.5 |
| | | Protein ubiquitination | | | | | |
| C9 | Q9UL46 | Proteasome activator complex subunit 2 | PSME2 | | 27.2−**27.3** | 5.4−**5.4** | −3.2 |
| C10 | Q06323 | Proteasome activator complex subunit 1 | PSME1 | 38 (9) | 28.7−**26.4** | 5.8−**5.8** | −2.3 |
| | | Intracellular transport | | | | | |
| T5 | Q9NP72 | Ras-related protein Rab-18 | RAB18 | 61 (10) | 22.7−**20.3** | 5.1−**5.0** | 4.4 |
| C6 | Q14847 | LIM and SH3 domain protein 1 | LASP1 | | 29.7−**36.4** | 6.6−**6.2** | −3.0 |
| | | Cytoskeleton organization | | | | | |
| T1 | Q13509 | Tubulin beta-3 chain | TUBB3 | 34 (10) | 50.4−**50.9** | 4.8−**4.9** | 4.2 |
| C8 | Q15691 | Microtubule-associated protein RP/EB family member 1 | MAPRE1 | 37 (6) | 29.9−**29.2** | 5.0−**5.0** | −5.6 |
| C12 | P43487 | Ran-specific GTPase-activating protein | RANBP1 | 11 (2) | 23.2−**24.8** | 5.2−**5.1** | −3.6 |
| C13 | P52566 | Rho GDP-dissociation inhibitor 2 | ARHGDIB | 26 (3) | 22.8−**23.6** | 5.1−**5.0** | −5.1 |

[a] UniProtKB/Swiss-Prot entry accession number (http://au.expasy.org). [b] Recommended gene name (official gene symbol) as provided by UniProtKB/Swiss-Prot. [c] Protein sequence coverage and number of signals matching the theoretical mass of tryptic peptides (C6 and C9 spot were identified only by MS/MS sequencing). [d] Theoretical values were calculated using Expasy Compute p$I$/$M_r$ tool (http://ca.expasy.org/tools/pi_tool.html) (signal peptides were not considered for $M_r$ and p$I$ calculations). Bold-faced numbers indicates $M_r$ and p$I$ experimental values. [e] Fold change (FC) of differentially regulated proteins [(−) down-regulated].

pression of intact B23/NPM protein (32.6 kDa) could not be determined by 2D gel image analysis; probably this protein spot was oversaturated, avoiding the detection of differential expression levels.

To increase the coverage of the proteome modulated by CIGB-300 in the nuclear fraction of NCI-H125 cells, a second comparative proteomic study using 2D-LC−MS/MS was performed. A total of 509 protein hits were identified (Supporting Information), of which 118 hits, corresponding to 127 proteins, were differentially expressed in CIGB-300-treated cells (Table 2). Interestingly, through this proteomic approach 12 of the 22 proteins identified by 2-DE analysis were also identified; the expression levels of these proteins were similarly modulated by CIGB-300 in both experiments (Table 2). Thus, such a finding serves as an internal cross-validation between both experimental approaches.

Changes in two differentially expressed proteins were validated through Western blot analysis of total cell extracts from NCI-H125 cells. CIGB-300 down-regulated the B23/NPM expression in a dose-dependent manner with the highest rate at 200 $\mu$M, the selected dose for proteomic studies (Figure 2). Although fragments of lowers apparent molecular weight from B23/NPM protein were not detected, the decreased expression of B23/NPM protein supported the detrimental effect of CIGB-300 on its stability. The increased expression of prohibitin (PHB) was also validated using the same experimental conditions. Similar to proteomic data, CIGB-300 up-regulated the PHB protein at 200 $\mu$M of CIGB-300; no significant effect was observed at lower peptide concentrations (Figure 2).

For better understanding of putative cellular processes affected by CIGB-300 on this lung cancer cell line, the differentially expressed proteins were classified in terms of their biological functions using the information from the Gene Ontology database. A considerable number of the identified proteins were involved in translation (23%), cytoskeleton organization (18%), RNA processing (11%), and apoptosis (7%) (Figure 3). Pathway analysis demonstrated the enrichment of metabolic, cytoskeletal signaling, translation, and gene expres-

**Table 2.** Differentially Expressed Proteins in NCI-H125 Cells Treated with CIGB-300, Identified Using 2D-LC−MS/MS

| protein hit | IPI_ACC[a] | UniProt_ACC[a] | description | gene symbol[b] | % coverage (peptides)[c] | FC[d] |
|---|---|---|---|---|---|---|
| | | | Translation | | | |
| 8 | IPI00008529 | P05387 | 60S acidic ribosomal protein P2 | RPLP2 | 63.48 (5) | 2 |
| 11 | IPI00181728 | Q8TDN6 | Brix domain-containing protein 2 | BXDC2 | 21.81 (3) | 2.7 |
| 12 | IPI00554723 | P27635 | 60S ribosomal protein L10 | RPL10 | 13.55 (2) | 2.7 |
| 14 | IPI00550021 | P39023 | 60S ribosomal protein L3 | RPL3 | 10.42 (3) | 7.2 |
| 15 | IPI00008530 | P05388 | 60S acidic ribosomal protein P0 | RPLP0 | 17.35 (2) | 2.7 |
| 17 | IPI00012772 | P62917 | 60S ribosomal protein L8 | RPL8 | 12.06 (2) | 9.6 |
| 19 | IPI00413324 | P18621 | 60S ribosomal protein L17 | RPL17 | 15.76 (3) | 2.9 |
| 21 | IPI00003918 | P36578 | 60S ribosomal protein L4 | RPL4 | 15.93 (4) | 2.6 |
| 22 | IPI00012795 | Q13347 | Eukaryotic translation initiation factor 3 subunit I | EIF3I | 24 (3) | 2 |
| 25 | IPI00745266 | Q9Y262 | Eukaryotic translation initiation factor 3 subunit L | EIF3L | 9.93 (3) | 2.2 |
| 29 | IPI00216587 | P62241 | 40S ribosomal protein S8 | RPS8 | 6.25 (1) | 12.1 |
| 30 | IPI00456758 | P46776 | 60S ribosomal protein L27a | RPL27A | 8.78 (1) | 3.1 |
| 31 | IPI00555744 | P50914 | 60S ribosomal protein L14 | RPL14 | 5.45 (1) | 3.7 |
| 34 | IPI00329389 | Q02878 | 60S ribosomal protein L6 | RPLl6 | 5.21 (1) | 9.2 |
| 43 | IPI00215719 | Q07020 | 60S ribosomal protein L18 | RPL18 | 6.91 (1) | 2.9 |
| 45 | IPI00221093 | P08708 | 40S ribosomal protein S17 | RPS17 | 7.41 (1) | 2.4 |
| 46 | IPI00008708 | O76021 | Ribosomal L1 domain-containing protein 1 | RSL1D1 | 4.08 (1) | 5 |
| 4 | IPI00025447 | Q6IQ15 | Elongation factor 1-alpha | EEF1A1 | 33.33 (9) | −2 |
| 6 | IPI00014424 | Q05639 | Elongation factor 1-alpha 2 | EEF1A2 | 34.34 (8) | −2 |
| 15 | IPI00008438 | P46783 | 40S ribosomal protein S10 | RPS10 | 32.73 (5) | −2.5 |
| 25 | IPI00013415 | P62081 | 40S ribosomal protein S7 | RPS7 | 27.32 (3) | −2.5 |
| 36 | IPI00783097 | P41250 | Glycyl-tRNA synthetase | GARS | 8.12 (3) | −3.3 |
| 38 | IPI00007074 | P54577 | Tyrosyl-tRNA synthetase, cytoplasmic | YARS | 10.61 (3) | −2.5 |
| 41 | IPI00816063<br>IPI00024933 | P30050 | Isoform 2 of 60S ribosomal protein L12<br>Isoform 1 of 60S ribosomal protein L12 | RPL12 | 14.39 (1)<br>11.52 (1) | OFF |
| 46 | IPI00295400<br>IPI00412737 | P23381 | Tryptophanyl-tRNA synthetase, cytoplasmic<br>Tryptophanyl-tRNA synthetase isoform b | WARS | 4.03 (1)<br>4.42 (1) | −5 |
| 50 | IPI00329633 | P26639 | Threonyl-tRNA synthetase, cytoplasmic | TARS | 8.85 (3) | −3.3 |
| 52 | IPI00300074 | Q9NSD9 | Phenylalanyl-tRNA synthetase beta chain | FARSB | 5.43 (2) | −2 |
| 53 | IPI00031820 | Q9Y285 | Phenylalanyl-tRNA synthetase alpha chain | FARSA | 4.72 (1) | −2 |
| 55 | IPI00215780 | P39019 | 40S ribosomal protein S19 | RPS19 | 10.34 (2) | −3.3 |
| 69 | IPI00032635<br>IPI00471933 | Q9BX40 | Isoform 1 of Protein LSM14 homologue B<br>Isoform 3 of Protein LSM14 homologue B | LSM14B | 6.75 (1)<br>10.88 (1) | −3.3 |
| 71 | IPI00375127<br>IPI00014263 | Q15056 | Similar to mKIAA0038 protein<br>Isoform Long of Eukaryotic translation initiation factor 4H | EIF4H | 7.82 (2)<br>9.27 (2) | −3.3 |
| | | | Apoptosis | | | |
| 35 | IPI00000816 | P62258 | 14−3−3 protein epsilon | YWHAE | 16.08 (2) | 2.6 |
| 17 | IPI00025512 | P04792 | Heat shock protein beta-1 | HSPB1 | 33.66 (3) | −3.3 |
| 21 | IPI00218733 | **P00441** | Superoxide dismutase [Cu−Zn] | SOD1 | 44.81 (2) | OFF |
| 26 | IPI00003815 | **P52565** | Rho GDP-dissociation inhibitor 1 | ARHGDIA | 24.02 (2) | −10 |
| 37 | IPI00550900 | **P13693** | Translationally controlled tumor protein | TCTP | 15.12 (2) | −3.3 |
| 40 | IPI00220766 | **Q04760** | Lactoylglutathione lyase | GLO1 | 20.65 (2) | −5 |
| 64 | IPI00026260 | P22392 | Isoform 1 of Nucleoside diphosphate kinase B | NME2 | 9.87 (1) | −2.5 |
| | IPI00795292 | | Isoform 3 of Nucleoside diphosphate kinase B | | 5.62 (1) | |
| 72 | IPI00219757 | **P09211** | Glutathione S-transferase P | GSTP1 | 9.52 (2) | −10 |
| | | | Cell proliferation | | | |
| 16 | IPI00441473 | O14744 | Protein arginine N-methyltransferase 5 | PRMT5 | 15.70 (6) | 2 |
| 32 | IPI00032406 | **O60884** | DnaJ homologue subfamily A member 2 | DNAJA2 | 7.04 (1) | 2.8 |
| 33 | IPI00395865 | Q16576 | Histone-binding protein RBBP7 | RBBP7 | 12 (2) | 2.3 |
| 44 | IPI00013953 | Q9NNW5 | WD repeat-containing protein 6 | WDR6 | 1.25 (1) | 4.2 |
| 20 | IPI00020956 | P51858 | Hepatoma-derived growth factor | HDGF | 18.33 (2) | −2 |
| 22 | IPI00014197<br>IPI00798278 | Q9UKY7 | Isoform 1 of Protein CDV3 homologue<br>Isoform 2 of Protein CDV3 homologue | CDV3 | 31.40 (2)<br>38.03 (2) | OFF |
| 30 | IPI00307226 | P01588 | Erythropoietin | EPO | 12.44 (2) | OFF |
| | | | Glucose catabolic process | | | |
| 1 | IPI00219018 | P04406 | Glyceraldehyde-3-phosphate dehydrogenase | GAPDH | 71.94 (16) | −10 |
| 2 | IPI00479186<br>IPI00220644 | P14618 | Isoform M2 of Pyruvate kinase isozymes M1/M2<br>Isoform M1 of Pyruvate kinase isozymes M1/M2 | PKM2 | 54.24 (17)<br>51.04 (15) | −10 |
| 3 | IPI00465439 | P04075 | Fructose-bisphosphate aldolase A | ALDOA | 43.96 (8) | −10 |
| 5 | IPI00169383 | P00558 | Phosphoglycerate kinase 1 | PGK1 | 35.49 (9) | −5 |
| 7 | IPI00027497 | P06744 | Glucose-6-phosphate isomerase | GPI | 29.03 (8) | −10 |
| 8 | IPI00451401<br>IPI00797270 | **P60174** | Isoform 2 of Triosephosphate isomerase<br>Isoform 1 of Triosephosphate isomerase | TPI1 | 35.74 (6)<br>47.39 (7) | −10 |
| 9 | IPI00607708<br>IPI00217966 | P00338 | Isoform 2 of L-lactate dehydrogenase A chain<br>L-lactate dehydrogenase | LDHA | 33.43 (6)<br>30.75 (6) | −10 |
| 16 | IPI00219217 | **P07195** | L-lactate dehydrogenase B chain | LDHB | 14.37 (4) | −5 |
| 44 | IPI00916111 | P40925 | Malate dehydrogenase | MDH1 | 9.38 (2) | −2.5 |
| 65 | IPI00219525 | P52209 | 6-phosphogluconate dehydrogenase, decarboxylating | PGD | 3.93 (1) | −5 |
| | | | RNA processing | | | |
| 23 | IPI00026089 | O75533 | Splicing factor 3B subunit 1 | SF3B1 | 3.53 (3) | 2 |
| 24 | IPI00217686 | Q8IY81 | Putative rRNA methyltransferase 3 | FTSJ3 | 5.43 (2) | 6.8 |
| | IPI00218592 | | Isoform ASF-3 of Splicing factor, arginine/serine-rich 1 | | 21.39 (2) | |
| 27 | IPI00215884 | Q07955 | Isoform ASF-1 of Splicing factor, arginine/serine-rich 1 | SFRS1 | 17.34 (2) | 2 |
| | IPI00218591 | | Isoform ASF-2 of Splicing factor, arginine/serine-rich 1 | | 14.73 (2) | |

**Table 2.** Continued

| protein hit | IPI_ACC[a] | UniProt_ACC[a] | description | gene symbol[b] | % coverage (peptides)[c] | FC[d] |
|---|---|---|---|---|---|---|
| 36 | IPI00003377 | Q16629 | Isoform 1 of Splicing factor, arginine/serine-rich 7 | SFRS7 | 8.82 (1) | 3.1 |
| | IPI00790699 | | Isoform 3 of U2-associated protein SR140 | | 2.91 (2) | |
| 40 | IPI00143753 | O15042 | Isoform 1 of U2-associated protein SR140 | SR140 | 2.82 (2) | 2.3 |
| | IPI00829908 | | Isoform 2 of U2-associated protein SR140 | | 2.82 (2) | |
| | IPI00215965 | | Isoform A1-B of Heterogeneous nuclear ribonucleoprotein A1 | | 24.73 (7) | |
| 10 | IPI00797148 | P09651 | Isoform 2 of Heterogeneous nuclear ribonucleoprotein A1 | HNRNPA1 | 34.46 (7) | −3.3 |
| | IPI00465365 | | Isoform A1-A of Heterogeneous nuclear ribonucleoprotein A1 | | 28.75 (7) | |
| | IPI00644968 | P0C7M2 | Putative heterogeneous nuclear ribonucleoprotein A1-like protein 3 | HNRPA1L3 | 28.75 (7) | |
| 11 | IPI00414696 | P22626 | Isoform A2 of Heterogeneous nuclear ribonucleoproteins A2/B1 | HNRNPA2B1 | 33.14 (7) | −2 |
| | IPI00396378 | | Isoform B1 of Heterogeneous nuclear ribonucleoproteins A2/B1 | | 32.01 (7) | |
| 24 | IPI00179964 | P26599 | Isoform 1 of Polypyrimidine tract-binding protein 1 | PTBP1 | 15.82 (4) | −2.5 |
| | IPI00334175 | | Isoform 2 of Polypyrimidine tract-binding protein 1 | | 15.27 (4) | |
| | IPI00412714 | | Isoform 4 of Plasminogen activator inhibitor 1 RNA-binding protein | | 11.89 (2) | |
| 27 | IPI00470497 | Q8NC51 | Isoform 2 of Plasminogen activator inhibitor 1 RNA-binding protein | SERBP1 | 3.98 (1) | −5 |
| | IPI00470498 | | Isoform 3 of Plasminogen activator inhibitor 1 RNA-binding protein | | 11.70 (2) | |
| | IPI00410693 | | Isoform 1 of Plasminogen activator inhibitor 1 RNA-binding protein | | 3.92 (1) | |
| 54 | IPI00328840 | Q86V81 | THO complex 4 | THOC4 | 9.85 (1) | −3.3 |
| 58 | IPI00003438 | O75937 | DnaJ homologue subfamily C member 8 | DNAJC8 | 11.46 (1) | −5 |
| 59 | IPI00299000 | Q9UQ80 | Proliferation-associated protein 2G4 | PA2G4 | 8.12 (2) | −2 |
| | | | Regulation of transcription | | | |
| 20 | IPI00513773 | Q6NZI2 | Isoform 2 of Polymerase I and transcript release factor | PTRF | 14.33 (2) | 2.4 |
| | IPI00176903 | | Isoform 1 of Polymerase I and transcript release factor | | 11.03 (2) | |
| 31 | IPI00872855 | Q01844 | RNA-binding protein EWS | EWSR1 | 6.40 (2) | −2.5 |
| 34 | IPI00853059 | Q96AE4 | Isoform 2 of Far upstream element-binding protein 1 | FUBP1 | 9.17 (3) | −5 |
| | IPI00375441 | | Isoform 1 of Far upstream element-binding protein 1 | | 6.06 (2) | |
| 42 | IPI00234252 | Q92922 | SWI/SNF complex subunit SMARCC1 | SMARCC1 | 3.17 (2) | −10 |
| 45 | IPI00031812 | P67809 | Nuclease-sensitive element-binding protein 1 | YBX1 | 9.26 (1) | −3.3 |
| 67 | IPI00171798 | O94776 | Metastasis-associated protein MTA2 | MTA2 | 4.64 (1) | OFF |
| | | | DNA replication | | | |
| 60 | IPI00413611 | P11387 | DNA topoisomerase 1 | TOP1 | 3.66 (2) | −2 |
| 70 | IPI00292858 | P19971 | Thymidine phosphorylase | TYMP | 3.11 (1) | −3.3 |
| | | | Protein ubiquitination | | | |
| 39 | IPI00384051 | **Q9UL46** | Proteasome activator complex subunit 2 | PSME2 | 12.85 (2) | −2.5 |
| 48 | IPI00645078 | P22314 | Ubiquitin-like modifier-activating enzyme 1 | UBA1 | 2.36 (2) | −2.5 |
| 51 | IPI00395627 | Q9HB71 | Isoform 1 of Calcyclin-binding protein | CACYBP | 9.21 (1) | −5 |
| 62 | IPI00479722 | **Q06323** | Proteasome activator complex subunit 1 | PSME1 | 9.24 (1) | −3.3 |
| 63 | IPI00029623 | P60900 | Proteasome subunit alpha type-6 | PSMA6 | 7.32 (1) | −5 |
| 68 | IPI00219913 | P54578 | Ubiquitin carboxyl-terminal hydrolase 14 | USP14 | 5.87 (1) | −3.3 |
| | | | Proteolysis | | | |
| 32 | IPI00011229 | P07339 | Cathepsin D | CTSD | 10.19 (3) | −3.3 |
| 61 | IPI00026216 | P55786 | Puromycin-sensitive aminopeptidase | NPEPPS | 3.16 (2) | −2 |
| | | | Intracellular transport | | | |
| 26 | IPI00001639 | Q14974 | Importin subunit beta-1 | KPNB1 | 5.37 (3) | 2 |
| 39 | IPI00017376 | Q15437 | Protein transport protein Sec23B | SEC23B | 3 (1) | 2.2 |
| 12 | IPI00010154 | P31150 | Rab GDP dissociation inhibitor alpha | GDI1 | 4.47 (2) | −5 |
| | IPI00645255 | Q5SX87 | GDP dissociation inhibitor 2 | GDI2 | 25.10 (5) | |
| 23 | IPI00303882 | O60664 | Isoform B of Mannose-6-phosphate receptor-binding protein 1 | M6PRBP1 | 20.74 (4) | −5 |
| | IPI00106668 | | Isoform A of Mannose-6-phosphate receptor-binding protein 1 | | 29.88 (3) | −10 |
| 33 | IPI00643041 | P62826 | GTP-binding nuclear protein Ran | RAN | 14.81 (2) | −3.3 |
| | | | Cytoskeleton organization | | | |
| 1 | IPI00556012 | Q5BKV1 | Myosin, heavy chain 9, nonmuscle | MYH9 | 43.58 (9) | 2 |
| 2 | IPI00007752 | P68371 | Tubulin beta-2C chain | TUBB2C | 55.06 (16) | 2.4 |
| 3 | IPI00909140 | P07437 | Tubulin beta chain | TUBB | 54.96 (10) | 2.8 |
| 4 | IPI00013475 | Q13885 | Tubulin beta-2A chain | TUBB2A | 36.18 (11) | 2.5 |
| | IPI00031370 | Q9BVA1 | Tubulin beta-2B chain | TUBB2B | | |
| 5 | IPI00013683 | **Q13509** | Tubulin beta-3 chain | TUBB3 | 44.89 (12) | 2.7 |
| | IPI00180675 | Q71U36 | Tubulin alpha-1A chain | TUBA1A | 39.25 (13) | |
| 6 | IPI00218343 | Q9BQE3 | Tubulin alpha-1C chain | TUBA1C | 33.41 (12) | 2.3 |
| | IPI00930688 | P68363 | Tubulin alpha-1B chain | TUBA1B | 42.35 (14) | |
| 7 | IPI00646779 | Q9BUF5 | Tubulin beta-6 chain | TUBB6 | 19.69 (6) | 2.8 |
| 9 | IPI00292496 | Q3ZCM7 | Tubulin beta-8 chain | TUBB8 | 10.59 (3) | 2.3 |
| | IPI00397526 | | Isoform 1 of Myosin-10 | | 6.02 (8) | |
| 10 | IPI00790503 | P35580 | Isoform 3 of Myosin-10 | MYH10 | 5.96 (8) | 2.1 |
| | IPI00479307 | | Isoform 2 of Myosin-10 | | 5.97 (8) | |
| 18 | IPI00017454 | Q9H853 | Putative tubulin-like protein alpha-4B | TUBA4B | 10.79 (2) | 2 |
| | IPI00220573 | P19105 | Myosin regulatory light chain 12A | MYL12A | 10.53 (1) | |
| 28 | IPI00033494 | O14950 | Myosin regulatory light chain 12B | MYL12B | 10.47 (1) | 2 |
| | IPI00220278 | P24844 | Myosin regulatory light polypeptide 9 | MYL9 | 10.47 (1) | |
| 41 | IPI00335168 | P60660 | Myosin light polypeptide 6 | MYL6 | 10.60 (1) | 2.3 |
| 18 | IPI00216691 | P07737 | Profilin-1 | PFN1 | 55.71 (4) | −3.3 |
| 28 | IPI00843975 | P15311 | Ezrin | EZR | 7.17 (3) | −5 |

**Table 2.** Continued

| protein hit | IPI_ACC[a] | UniProt_ACC[a] | description | gene symbol[b] | % coverage (peptides)[c] | FC[d] |
|---|---|---|---|---|---|---|
| 35 | IPI00419979 | Q13177 | Serine/threonine-protein kinase PAK 2 | PAK2 | 5.90 (1) | −10 |
| 43 | IPI00012011 | P23528 | Cofilin-1 | CFL1 | 25.30 (2) | −10 |
| 49 | IPI00028091 | P61158 | Actin-related protein 3 | ACTR3 | 12.20 (2) | −3.3 |
| 57 | IPI00003817 | **P52566** | Rho GDP-dissociation inhibitor 2 | ARHGDIB | 12.44 (1) | OFF |
| | | | Cell adhesion | | | |
| 42 | IPI00025861 | P12830 | Cadherin-1 | CDH1 | 2.27 (1) | 2.1 |
| | | | Others | | | |
| 13 | IPI00215637 | O00571 | ATP-dependent RNA helicase DDX3X | DDX3X | 13.60 (5) | 2.0 |
| | IPI00293616 | O15523 | ATP-dependent RNA helicase DDX3Y | DDX3Y | 10.30 (4) | |
| 37 | IPI00376379 | Q7Z794 | Keratin, type II cytoskeletal 1b | KRT77 | 4.67 (2) | 2.4 |
| 38 | IPI00021304 | P35908 | Keratin, type II cytoskeletal 2 epidermal | KRT2 | 4.19 (2) | 2.6 |
| 13 | IPI00003865 | P11142 | Isoform 1 of Heat shock cognate 71 kDa protein | HSPA8 | 14.86 (8) | −2 |
| 14 | IPI00792641 | B3KSI4 | Transketolase isoform 2 | TKT | 18.70 (5) | −5 |
| | IPI00643920 | B4DE31 | cDNA FLJ54957, highly similar to Transketolase | | 16.01 (5) | |
| 19 | IPI00746165 | O75083 | Isoform 1 of WD repeat-containing protein 1 | WDR1 | 16.17 (4) | −5 |
| 29 | IPI00289499 | P31939 | Bifunctional purine biosynthesis protein PURH | ATIC | 10.30 (3) | −2.5 |
| 47 | IPI00465431 | P17931 | Galectin-3 | LGALS3 | 11.60 (2) | −2.5 |
| 56 | IPI00299977 | Q9NRX4 | 14 kDa phosphohistidine phosphatase | PHPT1 | 16.80 (1) | −2.0 |
| 66 | IPI00644196 | P36952 | Isoform 2 of Serpin B5 | SERPINB5 | 7.36 (1) | −2.5 |
| | IPI00783625 | | Isoform 1 of Serpin B5 | | 4.53 (1) | |

[a] Accession numbers in IPI (International Protein Index) (http://www.ebi.ac.uk/IPI) and UniProtKB/Swiss-Prot databases (http://au.expasy.org) The UniProt accession numbers highlighted in bold indicate those proteins (12) that were also identified by 2-DE analysis. [b] Recommended gene name (official gene symbol) as provided by UniProtKB/Swiss-Prot. [c] Protein sequence coverage and number of identified peptides. [d] Fold change (FC) of differentially regulated proteins [(−) down-regulated].

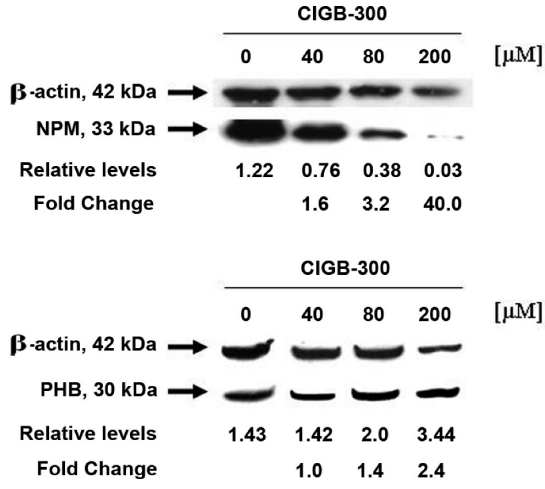


**Figure 2.** Validation of nucleophosmin (B23/NPM) and prohibitin (PHB) expression levels by Western blot analysis. NCI-H125 cells were treated with different concentrations of CIGB-300 during 40 min. Total cell lysates were separated on a SDS-PAGE gel and immunoblotting was performed with anti-B23/NPM and anti-PHB antibodies. $\beta$-Actin expression was used as control.

sion processes in the identified data set (Figure 4). Pathways are referred to according to annotations derived from different databases (Figure 4). Particularly, metabolic pathways are related to glycolysis and gluconeogenesis, whereas cytoskeletal proteins are mainly related to Gap junction and Rho GTPase signaling pathways.

Differentially expressed proteins related to the apoptosis process support the pro-apoptotic function of CIGB-300. Among these proteins, PHB is a negative regulator of cell proliferation that represses the E2F-mediated transcription pathway and activates the p53 transcriptional activity.[32,33] Thereby PHB has been described as a potential tumor suppressor protein. In this study, PHB expression was increased by CIGB-300 treatment (Table 1), such up-regulation was validated using Western blot analysis as referred above (Figure 2). Furthermore, a decrease of the translationally controlled tumor protein (TCTP) level was observed on CIGB-300 treated cells as confirmed through the two proteomic approaches used in this study (Table 1 and Table 2). TCTP is an antiapoptotic protein;[34] previous studies have demonstrated that down-regulation of TCTP is related with suppression of tumor malignant phenotype.[35]

From a mechanistic view, the down-regulation of B23/NPM protein induced by CIGB-300 is of great relevance (Figure 2). This nucleolar protein promotes cell survival through the inhibition of distinct pro-apoptotic pathways including the inactivation of the tumors suppressors IRF1 and p53.[36,37] Besides, B23/NPM regulates the ribosome biogenesis pathway by several mechanisms including the processing of pre-rRNA molecule in the internal transcribed spacer (ITS2) sequence to form the 5.8S and 28S rRNA.[38] In addition, B23/NPM elicits chaperone activity preventing protein aggregation at the nucleolus during ribosome assembly,[39] and mediating the nucleocytoplasmic transport of both ribosomal subunits.[40]

Besides B23/NPM, two other proteins related to ribosome biogenesis were down-regulated 2-fold in the presence of CIGB-300: DNA topoisomerase I (TOP1) and proliferation-associated protein 2G4 (PA2G4) (Table 2). TOP1 regulates rRNA transcription.[41] This protein catalyzes the transient breaking and rejoining of a single strand of DNA; such enzymatic function of TOP1 has been demonstrated to be activated by CK2 phosphorylation.[42] PA2G4 regulates the intermediate and late steps of rRNA processing and also contributes to maturation of the 60S ribosomal subunit.[43] Furthermore, PA2G4 represses the inhibitory phosphorylation of eukaryotic initiation factor 2 α (eIF2α), exerting as a consequence a positive regulation on protein translation.[44] In line with these findings, ribosomal proteins as well as different aminoacyl-tRNA synthetases were modulated by CIGB-300 treatment (Table 2, Figure 4). Ribosomal proteins failing to assemble into ribosome subunits undergo proteosomal degradation.[45] However, a set of proteins related to ubiquitin dependent degradation was down-regulated on CIGB-300-treated cells (Table 2). Therefore, the expected decrease of proteasome activity would explain the nuclear

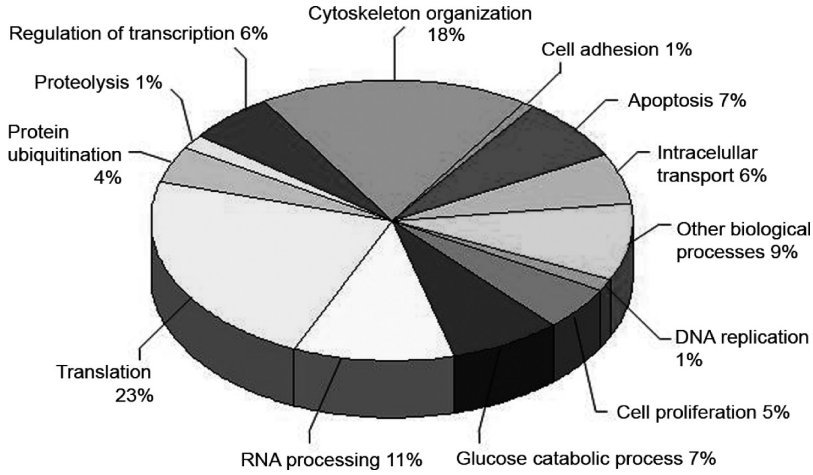


**Figure 3.** Distribution of the 137 proteins differentially expressed according to their biological functions.

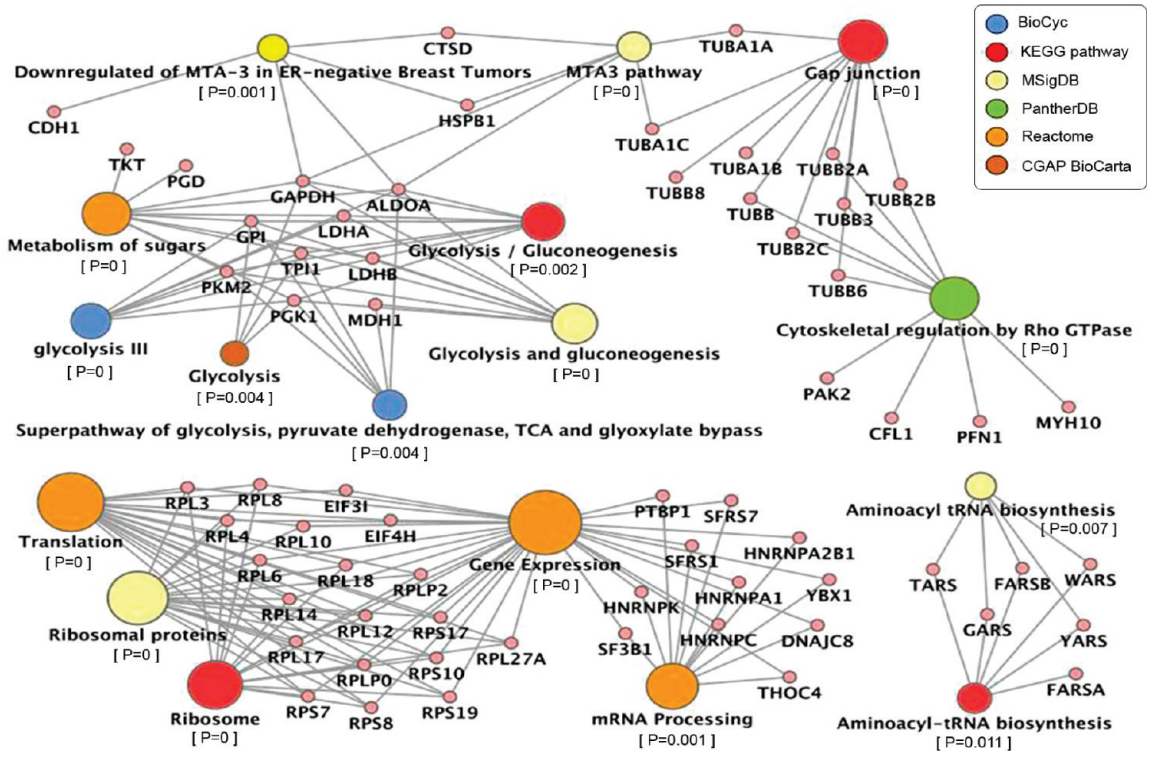


**Figure 4.** Pathways related to identified proteins. Nodes represent both pathways and proteins, and edges represent functional associations between them. The color of pathway nodes indicates the original data source, and the size is proportional to the number of identified proteins in each pathway according to ToppFun results. P-value of each pathway is given in brackets.

accumulation of ribosomal proteins observed in the presence of CIGB-300. Altogether, the inhibitory effect of CIGB-300 on B23/NPM stability, along with modulation of TOP1, PA2G4 and ribosomal proteins constitute experimental evidence supporting that CIGB-300 indeed impairs the ribosome biogenesis process.

Proteins that regulate cytoskeleton assembly and stability were identified in this study (Table 2, Figure 4). Particularly, ezrin, a protein important for cellular adhesion and migration[46] that has been implicated in growth and metastasis of several human cancers,[47−51] was down-regulated on CIGB-300-treated cells. In addition, the 14 kDa phosphohistidine phosphatase protein (PHPT1) that regulates cell migration and invasion of lung cancer cells through the cytoskeletal reorganization pathway[52] was also down-regulated by CIGB-300 (Table 2). The expression of Cadherin-1 (CDH1), a cell−cell adhesion glycoprotein considered as a negative regulator of cancer invasion,[53,54] was increased on CIGB-300-treated cells (Table 2). Therefore, the concomitant regulation of ezrin, PHPT1, and CDH1 suggests the inhibition of cellular motility in CIGB-300-treated cells.

In addition, other proteins related to metastasis were modulated on NCI-H125 cells by CIGB-300. Thymidine phosphorylase (TP) protein, which is an angiogenic factor that stimulates the chemotaxis of endothelial cells and also confers resistance to the hypoxia-induced apoptosis,[55,56] was down-regulated by CIGB-300 (Table 2). TP has been related to tumor invasion and metastasis in several cancers, such as cervical cancer and NSCLC.[57−60] The expression of Hepatoma-derived growth factor, a protein involved in anchorage-independent growth

and cell invasion of NSCLC,[61] was also decreased on CIGB-300-treated cells (Table 2). Furthermore, Glucose-6-phosphate isomerase, which functions as an extracellular cytokine stimulating cell motility,[62] was down-regulated by CIGB-300 (Table 2), while the Chromobox protein homologue 5, implicated in silencing metastasis-related genes,[63] was up-regulated on CIGB-300-treated cells (Table 1). Finally, the expression of Cathepsin D was decreased by CIGB-300 (Table 2). This protein regulates cell proliferation, invasion and metastasis.[64,65] Thus, the modulation of these proteins supports a potential antimetastasic effect of CIGB-300. Experiments in our lab are evaluating this hypothesis.

Cancer cells use glycolysis, even in aerobic conditions, to produce ATP and intermediaries metabolites for anabolic reactions.[66] Eight glycolytic proteins were down-regulated by CIGB-300 treatment in this study (Tables 1 and 2, Figure 4). Besides, the enzyme 6-phosphogluconate dehydrogenase, which catalyzes the third step of the pentose phosphate pathway oxidative branch, was down-regulated 5-fold by CIGB-300. The antioxidant defense system is essential for cancer cell survival.[67,68] The expression of the enzyme superoxide dismutase, which catalyzes the reduction of superoxide to hydrogen peroxide, was decreased on CIGB-300-treated cells (Tables 1 and 2). These results support the inhibitory effect of CIGB-300 on the proliferation of tumor cells. As the exacerbation of the glycolytic pathway has been considered an alternative way of tumor cells to resist chemotherapy,[69] our findings suggest that CIGB-300 could add a benefit to the standard anticancer therapies. In line with this hypothesis, Glutathione S-transferase P and Lactoylglutathione lyase, two glutathione conjugation proteins related to chemotherapy resistance,[70,71] were down-regulated on CIGB-300-treated NCI-H125 cells (Table 2). Additionally, the down-regulation of the Nuclease-sensitive element-binding protein 1 (YB-1) on CIGB-300-treated cells (Table 2) is of great importance as this factor activates the expression of the P-glycoprotein 1 coding gene related to the multidrug-resistant phenotype.[72,73] Furthermore, YB-1 participates in the nucleotide excision repair pathway and plays a role in the cisplatin-DNA adducts reparation.[74] This protein is overexpressed in cisplatin-resistant cells.[75] Besides the role of TP protein in metastasis, this protein, superoxide dismutase, and heat shock protein $\beta$-1 have been also related to cisplatin resistant phenotype on tumor cells.[76−79] These three proteins were down-regulated on CIGB-300-treated cells (Table 2). The findings observed in this study suggest that combination of CIGB-300 with some anticancer drugs may produce a synergistic interaction with increased overall antitumor effect.

## Conclusions

This study is the first proteomic analysis on cancer cells treated with the anticancer peptide CIGB-300. A total of 137 differentially expressed proteins were identified by two complementary proteomics approaches. CIGB-300 seems to promote the B23/NPM instability on NCI-H125 cells and the impairment of the ribosomal biogenesis and translation process. Such data are in line with previous findings demonstrating that CIGB-300 leads to apoptosis by blocking the CK2-mediated phosphorylation on B23/NPM with subsequent interference with the nucleolar assembly. Furthermore, other proteins implicated in apoptosis and cell proliferation were found modulated likely as a consequence from the above-mentioned effect of CIGB-300. These proteins could represent subrogate biomarkers of the CIGB-300 effect on tumor cells. Proteins related to glycolysis, antioxidant defense, angiogenesis, and metastasis were modulated on CIGB-300-treated cells, giving important clues about potential anticancer effects of CIGB-300 other than the pro-apoptotic action. CIGB-300 decreases the expression level of proteins implicated in chemotherapy resistance. Thus, such findings could support the combination of CIGB-300 with standard chemotherapeutic drugs to improve the antitumoral response. Overall, the dissection of the CIGB-300 modulated proteome not only documented the pathways supporting the demonstrated anticancer effect of CIGB-300 in lung cancer cells but also uncovered other potentialities of this drug for cancer therapy.

**Acknowledgment.** This work was supported by HeberBiotec SA and Biorec. The Proteomic and Bioinformatics Departments at the Center for Genetic Engineering and Biotechnology would like to thank to INSPUR Company (China) for their kind donation of a computer cluster used for data storage and processing.

**Supporting Information Available:** A complete table of identified proteins. This material is available free of charge via the Internet at http://pubs.acs.org.

## References

(1) Laramas, M.; Pasquier, D.; Filhol, O.; Ringeisen, F.; Descotes, J. L.; Cochet, C. *Eur. J. Cancer* **2007**, *43* (5), 928–934.
(2) Landesman-Bollag, E.; Romieu-Mourez, R.; Song, D. H.; Sonenshein, G. E.; Cardiff, R. D.; Seldin, D. C. *Oncogene* **2001**, *20* (25), 3247–3257.
(3) Kim, J. S.; Eom, J. I.; Cheong, J. W.; Choi, A. J.; Lee, J. K.; Yang, W. I.; Min, Y. H. *Clin. Cancer Res.* **2007**, *13* (3), 1019–1028.
(4) Daya-Makin, M.; Sanghera, J. S.; Mogentale, T. L.; Lipp, M.; Parchomchuk, J.; Hogg, J. C.; Pelech, S. L. *Cancer Res.* **1994**, *54* (8), 2262–2268.
(5) O-charoenrat, P.; Rusch, V.; Talbot, S. G.; Sarkaria, I.; Viale, A.; Socci, N.; Ngai, I.; Rao, P.; Singh, B. *Clin. Cancer Res.* **2004**, *10* (17), 5792–5803.
(6) Trembley, J. H.; Wang, G.; Unger, G.; Slaton, J.; Ahmed, K. *Cell. Mol. Life Sci.* **2009**, *66* (11−12), 1858–1867.
(7) Unger, G. M.; Davis, A. T.; Slaton, J. W.; Ahmed, K. *Curr. Cancer Drug Targets* **2004**, *4* (1), 77–84.
(8) Wang, G.; Unger, G.; Ahmad, K. A.; Slaton, J. W.; Ahmed, K. *Mol. Cell. Biochem.* **2005**, *274* (1−2), 77–84.
(9) Hung, M. S.; Xu, Z.; Lin, Y. C.; Mao, J. H.; Yang, C. T.; Chang, P. J.; Jablons, D. M.; You, L. *BMC Cancer* **2009**, *9*, 135.
(10) Sarno, S.; Reddy, H.; Meggio, F.; Ruzzene, M.; Davies, S. P.; Donella-Deana, A.; Shugar, D.; Pinna, L. A. *FEBS Lett.* **2001**, *496* (1), 44–48.
(11) Perea, S. E.; Reyes, O.; Puchades, Y.; Mendoza, O.; Vispo, N. S.; Torrens, I.; Santos, A.; Silva, R.; Acevedo, B.; Lopez, E.; Falcon, V.; Alonso, D. F. *Cancer Res.* **2004**, *64* (19), 7127–7129.
(12) Perea, S. E.; Reyes, O.; Baladron, I.; Perera, Y.; Farina, H.; Gil, J.; Rodriguez, A.; Bacardi, D.; Marcelo, J. L.; Cosme, K.; Cruz, M.; Valenzuela, C.; Lopez-Saura, P. A.; Puchades, Y.; Serrano, J. M.; Mendoza, O.; Castellanos, L.; Sanchez, A.; Betancourt, L.; Besada, V.; Silva, R.; Lopez, E.; Falcon, V.; Hernandez, I.; Solares, M.; Santana, A.; Diaz, A.; Ramos, T.; Lopez, C.; Ariosa, J.; Gonzalez, L. J.; Garay, H.; Gomez, D.; Gomez, R.; Alonso, D. F.; Sigman, H.; Herrera, L.; Acevedo, B. *Mol. Cell. Biochem.* **2008**, *316* (1−2), 163–167.
(13) Perera, Y.; Farina, H. G.; Hernandez, I.; Mendoza, O.; Serrano, J. M.; Reyes, O.; Gomez, D. E.; Gomez, R. E.; Acevedo, B. E.; Alonso, D. F.; Perea, S. E. *Int. J. Cancer* **2008**, *122* (1), 57–62.
(14) Solares, A. M.; Santana, A.; Baladron, I.; Valenzuela, C.; Gonzalez, C. A.; Diaz, A.; Castillo, D.; Ramos, T.; Gomez, R.; Alonso, D. F.; Herrera, L.; Sigman, H.; Perea, S. E.; Acevedo, B. E.; Lopez-Saura, P. *BMC Cancer* **2009**, *9*, 146.
(15) Perera, Y.; Farina, H. G.; Gil, J.; Rodriguez, A.; Benavent, F.; Castellanos, L.; Gomez, R. E.; Acevedo, B. E.; Alonso, D. F.; Perea, S. E. *Mol. Cancer Ther.* **2009**, Epub ahead of print. DOI:, 10.1158/1535-7163.MCT-08-1056.
(16) Fields, G. B.; Noble, R. L. *Int. J. Pept. Protein Res.* **1990**, *35* (3), 161–214.
(17) Klose, J.; Kobalz, U. *Electrophoresis* **1995**, *16* (6), 1034–1059.

(18) Heukeshoven, J.; Dernick, R. *J. Chromatogr.* **1985**, *326*, 91–101.
(19) Jensen, O. N.; Wilm, M.; Shevchenko, A.; Mann, M. Sample preparation methods for mass spectrometric peptide mapping directly from 2-DE gels. In *2-D Proteome Analysis Protocols*; Link, A. J., Ed.; Human Press: Totowa, NJ, 1999; pp 513−530.
(20) Gharahdaghi, F.; Weinberg, C. R.; Meagher, D. A.; Imai, B. S.; Mische, S. M. *Electrophoresis* **1999**, *20* (3), 601–605.
(21) Gonzalez, L. J.; Castellanos-Serra, L.; Badock, V.; Diaz, M.; Moro, A.; Perea, S.; Santos, A.; Paz-Lago, D.; Otto, A.; Muller, E. C.; Kostka, S.; Wittmann-Liebold, B.; Padron, G. *Electrophoresis* **2003**, *24* (1−2), 237–252.
(22) Perkins, D. N.; Pappin, D. J.; Creasy, D. M.; Cottrell, J. S. *Electrophoresis* **1999**, *20* (18), 3551–3567.
(23) Elias, J. E.; Gygi, S. P. *Nat. Methods* **2007**, *4* (3), 207–214.
(24) Fernandez-de-Cossio, J.; Gonzalez, L. J.; Satomi, Y.; Betancourt, L.; Ramos, Y.; Huerta, V.; Amaro, A.; Besada, V.; Padron, G.; Minamino, N.; Takao, T. *Nucleic Acids Res.* **2004**, *32* (Web Server issue), W674–W678.
(25) Fernandez-de-Cossio, J.; Gonzalez, L. J.; Satomi, Y.; Betancourt, L.; Ramos, Y.; Huerta, V.; Besada, V.; Padron, G.; Minamino, N.; Takao, T. *Rapid Commun. Mass Spectrom.* **2004**, *18* (20), 2465–2472.
(26) Dennis, G., Jr.; Sherman, B. T.; Hosack, D. A.; Yang, J.; Gao, W.; Lane, H. C.; Lempicki, R. A. *Genome Biol* **2003**, *4* (5), 3.
(27) Huang, d. W.; Sherman, B. T.; Lempicki, R. A. *Nat. Protoc.* **2009**, *4* (1), 44–57.
(28) Chen, J.; Bardes, E. E.; Aronow, B. J.; Jegga, A. G. *Nucleic Acids Res.* **2009**, *37* (Web Server issue), W305–W311.
(29) Shannon, P.; Markiel, A.; Ozier, O.; Baliga, N. S.; Wang, J. T.; Ramage, D.; Amin, N.; Schwikowski, B.; Ideker, T. *Genome Res.* **2003**, *13* (11), 2498–2504.
(30) Demalte-Annessi, I.; Sanchez, J.-C.; Hoogland, C.; Rouge, V.; Binz, P.-A.; Appel, R. D.; Hochstrasser, D. F. SWISS-2DPAGE database entry. http://www.expasy.org/swiss-2dpage/protein/ac=Q14847 (accessed Apr, 2010).
(31) Tawfic, S.; Olson, M. O.; Ahmed, K. *J. Biol. Chem.* **1995**, *270* (36), 21009–21015.
(32) Wang, S.; Zhang, B.; Faller, D. V. *EMBO J.* **2002**, *21* (12), 3019–3028.
(33) Fusaro, G.; Dasgupta, P.; Rastogi, S.; Joshi, B.; Chellappan, S. *J. Biol. Chem.* **2003**, *278* (48), 47853–47861.
(34) Liu, H.; Peng, H. W.; Cheng, Y. S.; Yuan, H. S.; Yang-Yen, H. F. *Mol. Cell. Biol.* **2005**, *25* (8), 3117–3126.
(35) Tuynder, M.; Susini, L.; Prieur, S.; Besse, S.; Fiucci, G.; Amson, R.; Telerman, A. *Proc. Natl. Acad. Sci. U.S.A.* **2002**, *99* (23), 14976–14981.
(36) Kondo, T.; Minamino, N.; Nagamura-Inoue, T.; Matsumoto, M.; Taniguchi, T.; Tanaka, N. *Oncogene* **1997**, *15* (11), 1275–1281.
(37) Li, J.; Zhang, X.; Sejas, D. P.; Bagby, G. C.; Pang, Q. *J. Biol. Chem.* **2004**, *279* (40), 41275–41279.
(38) Savkur, R. S.; Olson, M. O. *Nucleic Acids Res.* **1998**, *26* (19), 4508–4515.
(39) Szebeni, A.; Hingorani, K.; Negi, S.; Olson, M. O. *J. Biol. Chem.* **2003**, *278* (11), 9107–9115.
(40) Ahlemann, M.; Zeidler, R.; Lang, S.; Mack, B.; Munz, M.; Gires, O. *Mol. Carcinog.* **2006**, *45* (12), 957–967.
(41) Christensen, M. O.; Barthelmes, H. U.; Boege, F.; Mielke, C. *J. Biol. Chem.* **2002**, *277* (39), 35932–35938.
(42) Durban, E.; Goodenough, M.; Mills, J.; Busch, H. *EMBO J.* **1985**, *4* (11), 2921–2926.
(43) Squatrito, M.; Mancino, M.; Donzelli, M.; Areces, L. B.; Draetta, G. F. *Oncogene* **2004**, *23* (25), 4454–4465.
(44) Squatrito, M.; Mancino, M.; Sala, L.; Draetta, G. F. *Biochem. Biophys. Res. Commun.* **2006**, *344* (3), 859–868.
(45) Lam, Y. W.; Lamond, A. I.; Mann, M.; Andersen, J. S. *Curr. Biol.* **2007**, *17* (9), 749–760.
(46) Pujuguet, P.; Del Maestro, L.; Gautreau, A.; Louvard, D.; Arpin, M. *Mol. Biol. Cell* **2003**, *14* (5), 2181–2191.
(47) Hunter, K. W. *Trends Mol. Med.* **2004**, *10* (5), 201–204.
(48) Osawa, H.; Smith, C. A.; Ra, Y. S.; Kongkham, P.; Rutka, J. T. *Neuro-Oncol.* **2009**, *11* (4), 381–393.
(49) Wang, H. J.; Zhu, J. S.; Zhang, Q.; Sun, Q.; Guo, H. *World J. Gastroenterol.* **2009**, *15* (16), 2016–2019.
(50) Li, Q.; Wu, M.; Wang, H.; Xu, G.; Zhu, T.; Zhang, Y.; Liu, P.; Song, A.; Gang, C.; Han, Z.; Zhou, J.; Meng, L.; Lu, Y.; Wang, S.; Ma, D. *Cancer Lett.* **2008**, *261* (1), 55–63.
(51) Xie, J. J.; Xu, L. Y.; Xie, Y. M.; Zhang, H. H.; Cai, W. J.; Zhou, F.; Shen, Z. Y.; Li, E. M. *Int. J. Cancer* **2009**, *124* (11), 2549–2558.
(52) Xu, A.; Hao, J.; Zhang, Z.; Tian, T.; Jiang, S.; Hao, J.; Liu, C.; Huang, L.; Xiao, X.; He, D. *Lung Cancer* **2010**, *67* (1), 48–56.
(53) Shibanuma, H.; Hirano, T.; Tsuji, K.; Wu, Q.; Shrestha, B.; Konaka, C.; Ebihara, Y.; Kato, H. *Lung Cancer* **1998**, *22* (2), 85–95.
(54) Kase, S.; Sugio, K.; Yamazaki, K.; Okamoto, T.; Yano, T.; Sugimachi, K. *Clin. Cancer Res.* **2000**, *6* (12), 4789–4796.
(55) Akiyama, S.; Furukawa, T.; Sumizawa, T.; Takebayashi, Y.; Nakajima, Y.; Shimaoka, S.; Haraguchi, M. *Cancer Sci.* **2004**, *95* (11), 851–857.
(56) Ikeda, R.; Tajitsu, Y.; Iwashita, K.; Che, X. F.; Yoshida, K.; Ushiyama, M.; Furukawa, T.; Komatsu, M.; Yamaguchi, T.; Shibayama, Y.; Yamamoto, M.; Zhao, H. Y.; Arima, J.; Takeda, Y.; Akiyama, S.; Yamada, K. *Biochem. Biophys. Res. Commun.* **2008**, *370* (2), 220–224.
(57) Takao, S.; Akiyama, S. I.; Nakajo, A.; Yoh, H.; Kitazono, M.; Natsugoe, S.; Miyadera, K.; Fukushima, M.; Yamada, Y.; Aikou, T. *Cancer Res.* **2000**, *60* (19), 5345–5348.
(58) Yu, E. J.; Lee, Y.; Rha, S. Y.; Kim, T. S.; Chung, H. C.; Oh, B. K.; Yang, W. I.; Noh, S. H.; Jeung, H. C. *Mol. Cancer Res.* **2008**, *6* (10), 1554–1566.
(59) Ueda, M.; Terai, Y.; Kumagai, K.; Ueki, K.; Kanemura, M.; Ueki, M. *Int. J. Cancer* **2001**, *91* (6), 778–782.
(60) Sato, J.; Sata, M.; Nakamura, H.; Inoue, S.; Wada, T.; Takabatake, N.; Otake, K.; Tomoike, H.; Kubota, I. *Int. J. Cancer* **2003**, *106* (6), 863–870.
(61) Zhang, J.; Ren, H.; Yuan, P.; Lang, W.; Zhang, L.; Mao, L. *Cancer Res.* **2006**, *66* (1), 18–23.
(62) Funasaka, T.; Haga, A.; Raz, A.; Nagase, H. *Int. J. Cancer* **2002**, *101* (3), 217–223.
(63) Kirschmann, D. A.; Lininger, R. A.; Gardner, L. M.; Seftor, E. A.; Odero, V. A.; Ainsztein, A. M.; Earnshaw, W. C.; Wallrath, L. L.; Hendrix, M. J. *Cancer Res.* **2000**, *60* (13), 3359–3363.
(64) Liaudet-Coopman, E.; Beaujouin, M.; Derocq, D.; Garcia, M.; Glondu-Lassis, M.; Laurent-Matha, V.; Prebois, C.; Rochefort, H.; Vignon, F. *Cancer Lett.* **2006**, *237* (2), 167–179.
(65) Vashishta, A.; Ohri, S. S.; Proctor, M.; Fusek, M.; Vetvicka, V. *Anticancer Res.* **2006**, *26* (6B), 4163–4170.
(66) Kroemer, G.; Pouyssegur, J. *Cancer Cell* **2008**, *13* (6), 472–482.
(67) Pelicano, H.; Carney, D.; Huang, P. *Drug Resist. Updates* **2004**, *7* (2), 97–110.
(68) Hileman, E. O.; Liu, J.; Albitar, M.; Keating, M. J.; Huang, P. *Cancer Chemother. Pharmacol.* **2004**, *53* (3), 209–219.
(69) Xu, R. H.; Pelicano, H.; Zhou, Y.; Carew, J. S.; Feng, L.; Bhalla, K. N.; Keating, M. J.; Huang, P. *Cancer Res.* **2005**, *65* (2), 613–621.
(70) Su, F.; Hu, X.; Jia, W.; Gong, C.; Song, E.; Hamar, P. *J. Surg. Res.* **2003**, *113* (1), 102–108.
(71) Antognelli, C.; Baldracchini, F.; Talesa, V. N.; Costantini, E.; Zucchi, A.; Mearini, E. *Cancer J.* **2006**, *12* (3), 222–228.
(72) Ohga, T.; Uchiumi, T.; Makino, Y.; Koike, K.; Wada, M.; Kuwano, M.; Kohno, K. *J. Biol. Chem.* **1998**, *273* (11), 5997–6000.
(73) Saji, H.; Toi, M.; Saji, S.; Koike, M.; Kohno, K.; Kuwano, M. *Cancer Lett.* **2003**, *190* (2), 191–197.
(74) Gaudreault, I.; Guay, D.; Lebel, M. *Nucleic Acids Res.* **2004**, *32* (1), 316–327.
(75) Yahata, H.; Kobayashi, H.; Kamura, T.; Amada, S.; Hirakawa, T.; Kohno, K.; Kuwano, M.; Nakano, H. *J. Cancer Res. Clin. Oncol.* **2002**, *128* (11), 621–626.
(76) Ikeda, R.; Furukawa, T.; Mitsuo, R.; Noguchi, T.; Kitazono, M.; Okumura, H.; Sumizawa, T.; Haraguchi, M.; Che, X. F.; Uchimiya, H.; Nakajima, Y.; Ren, X. Q.; Oiso, S.; Inoue, I.; Yamada, K.; Akiyama, S. *Biochem. Biophys. Res. Commun.* **2003**, *301* (2), 358–363.
(77) Hisano, T.; Ono, M.; Nakayama, M.; Naito, S.; Kuwano, M.; Wada, M. *FEBS Lett.* **1996**, *397* (1), 101–107.
(78) Hour, T. C.; Lai, Y. L.; Kuan, C. I.; Chou, C. K.; Wang, J. M.; Tu, H. Y.; Hu, H. T.; Lin, C. S.; Wu, W. J.; Pu, Y. S.; Sterneck, E.; Huang, A. M. *Biochem. Pharmacol.* **2010**, *80* (3), 325–34.
(79) Lee, J. H.; Sun, D.; Cho, K. J.; Kim, M. S.; Hong, M. H.; Kim, I. K.; Lee, J. S.; Lee, J. H. *J. Cancer Res. Clin. Oncol.* **2007**, *133* (1), 37–46.

PR100728V